Towards a method for quantitative evaluation of nanoparticle from suspensions via microarray printing and SEM analysis

Towards a method for quantitative evaluation of nanoparticle from suspensions via microarray printing and SEM analysis

F Bennet[1,3], L Burr[2], D Schmid[2], V-D Hodoroaba[1]

[1]Federal Institute for Materials Research and Testing (BAM), Berlin, Germany

[2]Swiss Center for Electronics and Microtechnology (CSEM), Landquart, Switzerland

[3]Current address: Federal Institute for Risk Assessment (BfR), Berlin, Germany

francesca.bennet@bfr.bund.de; dan.hodoroaba@bam.de

Abstract. As part of the development of a library of accurate and efficient methods for measurement of nanoparticle properties, we develop and optimize a method for the efficient analysis of nanoparticle size distribution from suspensions via microprinting and digital analysis of electron microscopy (SEM and TEM) images, with the ultimate aim of automated quantitative concentration analysis (calculated from drop volume). A series of different nanoparticle suspensions (gold, latex, and SiO_2 in varying sizes and concentrations) were printed onto TEM grids in a 4 x 4 array in the concentration range 7×10^8 to 1×10^{11} nanoparticles/mL and imaged with SEM. Concentrations and printing conditions (temperature, relative humidity) were varied in order to minimize the coffee-ring effect.

1. Introduction

Nanomaterials are being used in exponentially increasing quantities in technology and consumer products and are therefore increasingly coming in contact with both humans and the environment. A thorough understanding of their toxicological properties is thus becoming increasingly important. In order to reduce the potential laboratory workload for toxicological testing as well as minimize handling deviations, enabling effective classification, regulation and labelling of nanomaterials, a comprehensive understanding of the relationship between physico-chemical and toxicological properties is necessary. This situation then requires efficient and accurate measurement of the various physical and chemical properties of the nanoparticles (such as size, shape, aspect ratio, inner and surface chemistry) as well as an understanding of which properties have the strongest influence on their behavior. In addition to individual nanoparticle properties, factors such as nanoparticle size distribution and concentration are highly relevant for both performance and safety considerations. It is therefore necessary to develop a library of analytical methods which can provide reliable, reproducible, accurate and validated data. This is the goal of the H2020 ACEnano project within which this work was conducted [1].

Naturally, a library of analytical methods is most useful when the methods are as cheap, simple and easy to use. In addition to providing complete documentation, including background information and Standard Operation Procedures (SOPs) as part of the ACEnano project, method development should show a trend towards increased efficiency and automation. For the same reasons, method development

tends towards miniaturization, to minimize both sample and materials quantities required for the measurement. All these steps should finally not affect but support the reproducibility of the results.

As part of this goal, we develop and optimize a method for the efficient analysis of nanoparticle size distribution in suspension via microarray printing and digital analysis of scanning electron microscopy (SEM) or transmission electron microscopy (TEM) images, with the ultimate aim of automated quantitative concentration analysis (calculated from drop volume) additionally to the particle size distribution. This method requires consistent printing of microdroplets onto coated TEM grids in a single layer of isolated (i.e. not overlapping) particles, at sufficient concentrations to give a statistically significant number of particles in each electron microscopy (EM) image.

Coated TEM grids were chosen as a substrate as they are readily available, have a high and uniform quality, are suitable for microarray printing and allow both SEM and TEM analysis. Printing multiple drops on one TEM grid greatly increases the efficiency of analysis through a reduction in time taken to change samples, as well as increasing the accuracy of the method by allowing repeat samples, but requires accurate printing of the dots so that they lie on the carbon film between the grid and are then visible in both the SEM and TEM images.

With a lateral resolution in the range of nanometers or below, enabling visual imaging of individual nanoobjects, as well as the possibility for lateral calibration of the image and therefore accurate measurement of object size, electron microscopy is the most commonly used method for the analysis of nanoparticle morphology. The use of a high-resolution SEM allows measurement of nanoparticles with a resolution of a few nm. By employing either a transmission electron (STEM) detector or a dedicated sample holder, nanoparticles prepared on conventional TEM grids can be also analyzed in the same SEM chamber in transmission mode, similarly to STEM, but at low energies (<30 keV). We call this operation mode STEM-in-SEM or simply TSEM [2,3]. The choice of SEM or TSEM measurement from the identical region of interest on the sample is advantageous due to the complementarity of the different contrast types: SEM InLens being sensitive to the sample surface and TSEM being sensitive to the material density and/or thickness. Usually, by a single key press one has the pair of images SEM-InLens (taken from the top of the sample) and TSEM (collecting the transmitted electrons through the sample). One advantage of TSEM is the more accurate measurement of the lateral dimensions of nanoobjects, i.e. of nanoparticle size, due to the superior transmission contrast and hence, better definition of the particle boundaries.

In order to obtain useful EM images from the printed droplets several requirements must be met. First, the samples should be relatively free from impurities, such that the nanoparticles rather than impurities dominate the precipitated matter from the droplet. There are several methods available for purifying nanoparticles, including dialysis and centrifugation/re-dispersion with clean solvent [4]. However, purification may decrease particle suspension stability, thus the method development described in this work focused on conditions for maximum experimental efficiency with a minimum number of preparation steps. Second, the nanoparticles should be visible in high enough contrast to be easily distinguished by the image analysis software from the background and other impurities. Third, the nanoparticles should not form multilayers on the substrate, i.e. the sample should form a single layer with particles distinct from each other and not clumped together. Fourth, there should be a statistically significant number of particles in any image so that an accurate analysis of particle size distribution can be undertaken. Fifth, nanoparticles should ideally be present as single particles and largely free from aggregates or agglomerates, however the presence and size of aggregates and agglomerates can be of interest in the analysis. In that case it is important that the method is able to differentiate from nanoparticles aggregated and agglomerated in the dispersion, and particles that have simply been printed in a multilayer or group on top of one another. Finally, the uniform distribution of the nanoparticles across the droplet is crucial for the accurate evaluation of the nanoparticle concentration, calculated from the number of particles in the image area, measurement of the dried droplet diameter and knowledge of the printed drop volume. In order to achieve this, the elimination of the coffee-ring effect during drying is of high priority in the method development.

The "coffee-ring" effect is the commonly used name for the migration of particles or dissolved chemicals to the pinned sides of the droplet during drying, according to the Marangoni effect [5-9]. The elimination of this effect has been studied in-depth in literature, with various creative options applied [7,10-22]. In addition to the problem of concentration determination in this method, elimination of the coffee-ring effect is relevant to particle size distribution determination, since it has been shown to separate particles of different shape and size during drying [10,14,23-28]; the location of the EM image within the droplet is therefore crucial. For the development of a reliable, stable and effective analytical method, this inconsistency should be eliminated, and the coffee-ring effect reduced as much as possible. Further, the development of deposition of very small droplets on the substrate enables the quick measurement of all particles within the dried droplet even with no need for homogeneity of NP deposition.

When a droplet dries, the edges of the droplet are "pinned" to the substrate and do not move; the droplet diameter therefore remains static. Due to the restrictions imposed by the number of particles drying in a drop of a particular size, there is an upper limit to the concentration of nanoparticles that can be evaluated in a suspension using this method; if it is exceed, the nanoparticles do not have sufficient area to dry in single layers and the particle size cannot be readily evaluated using software.

2. Experimental

2.1. Materials

Ludox™ TM-40 colloidal SiO_2 nanoparticles (20 nm diameter) were obtained from Aldrich (Prod# 420786) in a 40 w% aqueous dispersion (about 7.00 $x10^{16}$ NP/mL). Polystyrene latex nanoparticles (100 nm diameter) were obtained from Polyscience (COOH Polybead® microsphere cat# 16688) in a 2.6 w% aqueous dispersion (about 4.55$x10^{13}$ NP/mL). Colloidal gold nanoparticles (20 and 200 nm, respectively) were obtained from BBI Solutions in aqueous dispersions with concentration of 7.00$x10^{11}$ and 7.00$x10^{8}$ NP/mL respectively. Nanoparticles were either used as received or diluted using MilliQ water (18.2 MΩ.cm – MilliPore – MilliQ Direct 8) with no further purification steps. Cu TEM grids coated with carbon film (Plano – SF162) were used as received as printing substrate. Hellmanex™ II detergent solution diluted to 5 v% (Hellma GmbH & Co. KG) and 2-propanol (HPLC grade, 99.9%, Sigma-Aldrich, Product N°: 34863-1L) were used for system cleaning and conditioning purposes.

2.2. Microarray printing

Printing on Cu TEM grids deposited on clean microscopy glass slide substrates was realized using a NanoPlotter 2.0 (GeSIM GmbH) piezo-electric printer equipped with Nano-Tip J piezoelectric pipette tips with nominal droplet volumes of 0.35-0.4 nL. Printing parameters (droplet volume, droplet speed, drop casting rate and printout drying) were optimized for each nanoparticle suspension. The final conditions of 400 pL droplets were printed in a 4x4 array, with each suspension printed in 4 spots and the grids printed in triplicate. Droplet drying parameters were varied, in the ranges of temperature (21-40 °C) and relative humidity (50-80%) within the enclosed evaporation chamber in which the droplets were printed.

A series of suspensions were printed with varying concentrations and under varying temperature and relative humidity, described in Table 1, to determine which parameters increased or reduced the coffee-ring effect, and to determine the optimum concentration range of the method.

	Size (nm)	Concentration (NP/mL)				
Au200	200	$7x10^8$	$7x10^8$	$7x10^8$	$7x10^8$	$7x10^8$
Latex	100	$1x10^{11}$	$5x10^{10}$	$1x10^{10}$	$1x10^9$	$1x10^9$
Au20	20	$1x10^{10}$	$5x10^{10}$	$1x10^{11}$	$1x10^9$	$1x10^9$
SiO_2	20	$1 x10^{11}$	$5x10^{10}$	$1x10^{10}$	$1x10^9$	$1x10^9$
T (°C)	**-**	**21**	**21**	**21**	**21**	**40**
Rel. Humidity (%)	**-**	**50**	**50**	**50**	**80**	**30**

Table 1. Concentrations and printing conditions for various nanoparticle suspensions

2.3. EM analysis and image evaluation

The printed TEM grids were imaged using a Zeiss Supra 40 scanning electron microscope (SEM) (Zeiss, Oberkochen, Germany) equipped with a Schottky field emitter as well as an InLens secondary electron detector. SEM and TSEM images were analysed using ImageJ software [29]. Images were converted to 8-bit greyscale images and analysed for the minimum Feret diameter using the NanoDefine Particle Sizer plugin.

3. Results

After the initial optimization steps for the printing process which are not documented in this publication, the various nanoparticle suspensions were printed at different concentrations and experimental conditions, with the following aims:

- Determine which conditions minimize the coffee ring effect
- Investigate if varying concentrations help to improve the printing quality
- Investigate if the printing is reproducible (all spots with the same number of particles)
- Investigate if the printing is quantitative (all spots with particle number proportional to the printed concentrations
- Determine the optimal printing concentration

Since the elimination or reduction of the coffee-ring effect to a reasonable level is a major parameter affecting the success of this method, it was the focus of much of the effort in the method optimization.

3.1. Accuracy of printing and droplet size

After optimisation of the initial conditions, droplets could be printed accurately on the TEM grid, with a small percentage (normally in the range 10-20%) of droplets incomplete or missing due to inaccurate printing or damage to the carbon film on the TEM grid.

The printed droplets mostly formed quasi-circular shapes, although some droplets were non-uniform in shape. A uniform circular shape is necessary for calculation of printed NP concentration from droplet volume and dried droplet size. Measured dried droplet sizes of SiO_2 NPs were also found to vary with suspension concentration and drying conditions (temperature and relative humidity), see Figure 1. This effect is not critical and was not investigated further, however it is important to consider when attempting to calculate NP concentration.

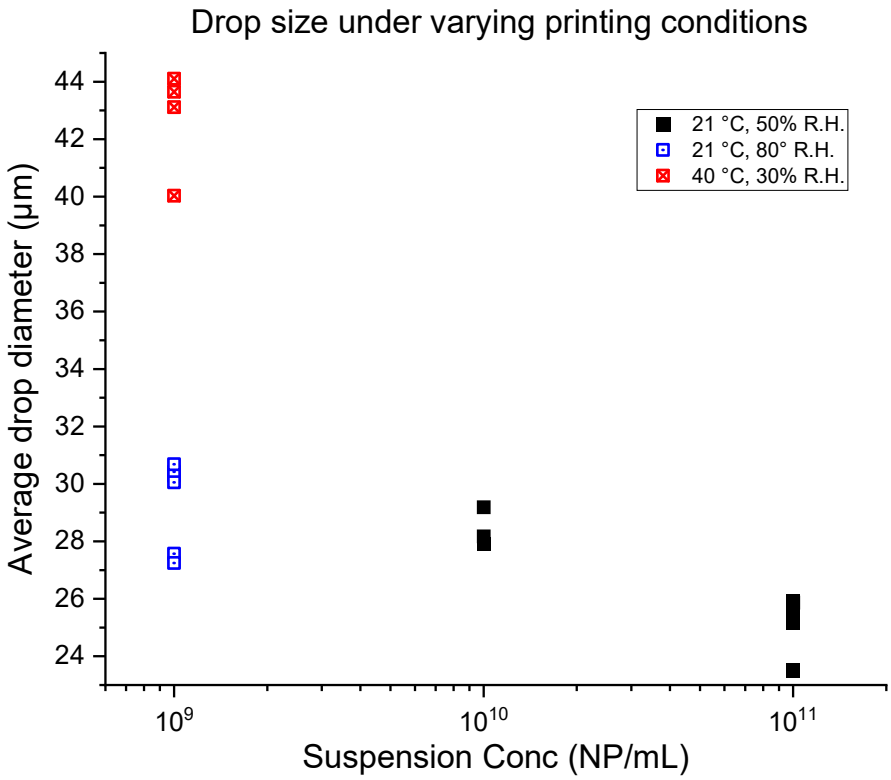

Figure 1: Measured droplet size for SiO_2 nanoparticle suspension, relative to suspension concentration and under varying experimental conditions

3.2. Results from different nanoparticle suspensions

The large difference in behaviour of the various NPs in this study can be seen in Figure 2. The gold samples, particularly the Au200 nanoparticles in Figure 2 (a) show large amounts of impurities which precipitate in concentric rings within the droplet. In addition, most of the gold seem to be present in large aggregates or agglomerates which appear extremely brightly in the SEM images and are therefore relatively easy to identify. This agglomeration/aggregation may be caused by ageing of the sample. While the high contrast of gold nanoparticles in SEM images makes this material a potentially ideal candidate for digital image evaluation, these results render the droplets unsuitable for further analysis. Further work was therefore focussed on droplets printed from latex and SiO_2 suspensions.

(a) 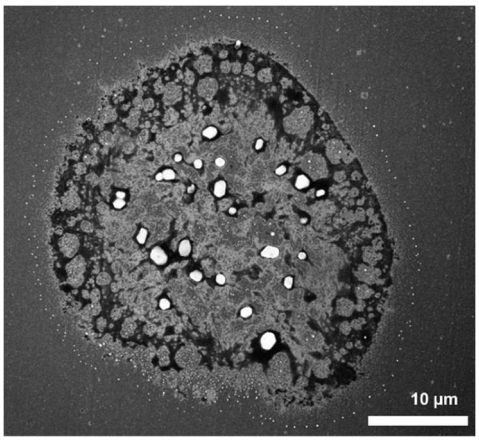

(b) 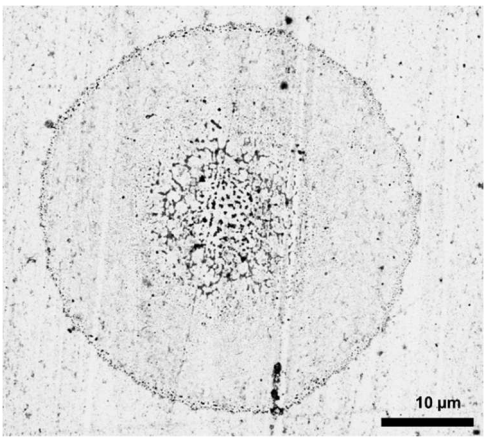

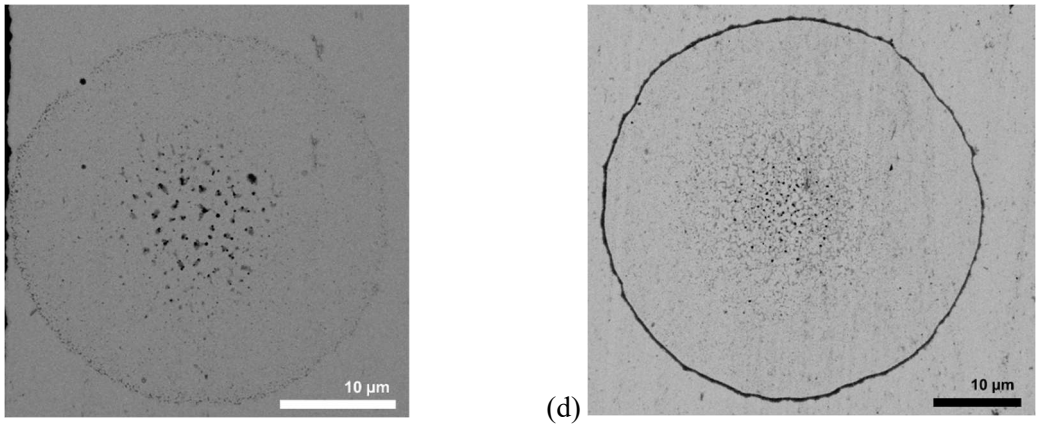

Figure 2: TSEM and SEM images, from printing at 40 °C and 30% R.H., of (a) Au200 ($7x10^8$ NP/mL); (b) Latex ($1x10^9$ NP/mL); (c) Au20 ($1x10^9$ NP/mL); (d) SiO_2 ($1x10^9$ NP/mL)

3.3. Coffee-ring effect and monolayer formation

The different materials in this study all show some propensity to form coffee-rings, with the effect being most pronounced for the latex and SiO_2 nanoparticles. This is likely due to the relative affinity of the particles with the substrate and with each other, which will be affected by the surface energy and hydrophilicity/hydrophobicity of the droplet and substrate as well as surface tension of the solvent.

The SiO_2 nanoparticles offer the best possibility for digital image evaluation from this technique. They form a monolayer in the middle of the droplet, even at higher concentrations, with the bulk of the particles appearing in the coffee-ring. At much lower concentrations, the nanoparticles form "islands" which are connected to each other although they mostly still appear in monolayers; the coffee-ring is still present, however to a much lesser extent, as shown in Figure 3. The formation of the monolayer even with a large coffee-ring effect as seen in Figure 3(a), combined with the effect seen in Figure 3 (b) of the breaking-up of the monolayer even with some nanoparticles collected in a pronounced coffee-ring, indicates two strongly competing effects.

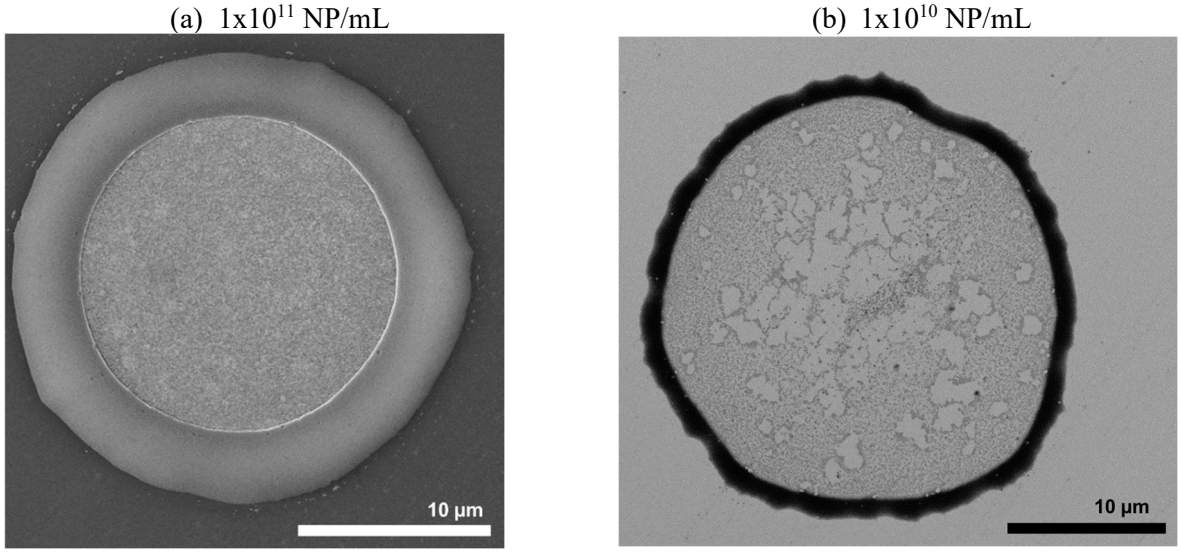

Figure 3: Effect of concentration on coffee-ring and monolayer formation from SiO_2 NPs printed at 21 °C and 50 % R.H.

Latex nanoparticles on the other hand have a much higher affinity for each other than for the substrate. They do not exhibit a similar strong tendency towards a continuous monolayer as seen with the SiO_2 and are much more prone to form multilayers even when there is insufficient material to form a continuous layer in the center of the dried droplet, see Figure 4.

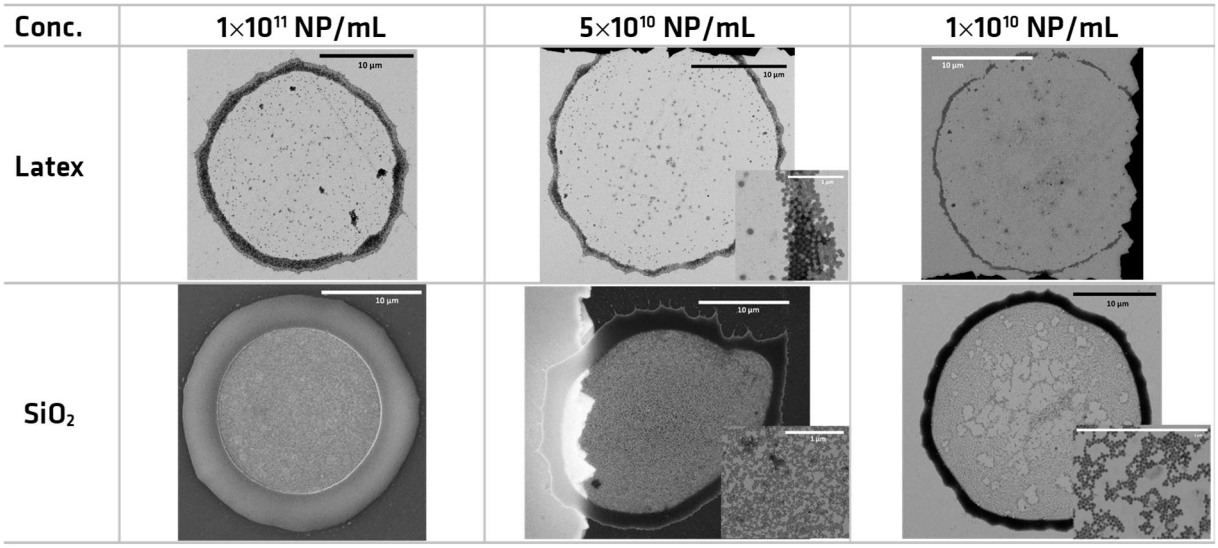

Figure 4: Comparison of the effect of concentration on coffee-ring and monolayer formation in SiO_2 and latex NPs printed at 21 °C and 50 % R.H. Scale bars in the droplet-sized images are 10 µm and in the zoomed-in images are 1 µm.

As seen, the concentration has little effect on the ability to form a continuous layer of sufficient density with the latex nanoparticles, in contrast to the SiO_2 nanoparticles. In addition, while the latex nanoparticles can be manually identified relatively easily, their low contrast (medium grey in images) combined with surrounding higher contrast (darker colour) impurities in the TSEM images make digital evaluation difficult, see Figure 5.

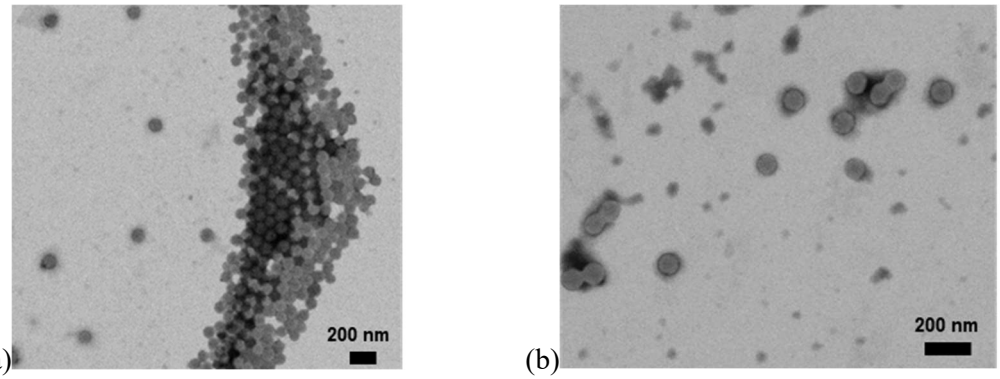

(a) (b)

Figure 5: The tendency of latex nanoparticles to form multilayers (a) as well as their low contrast due to surrounding impurities (b) make digital image evaluation difficult.

3.4. Reduction of the coffee-ring effect

In addition to changing concentration, the relative humidity and temperature of the printing environment were changed in order to reduce the coffee-ring effect. The conditions were varied in a temperature range of 21-40 °C and relative humidity (R.H.) range of 30-80 %, as shown in Figure 6. In the comparison between Figure 6(a) and Figure 6(b), lower temperature and higher relative humidity

leads to a clear decrease in the formation of coffee-rings [30-32] and correspondingly a better distribution of the nanoparticles across the droplet.

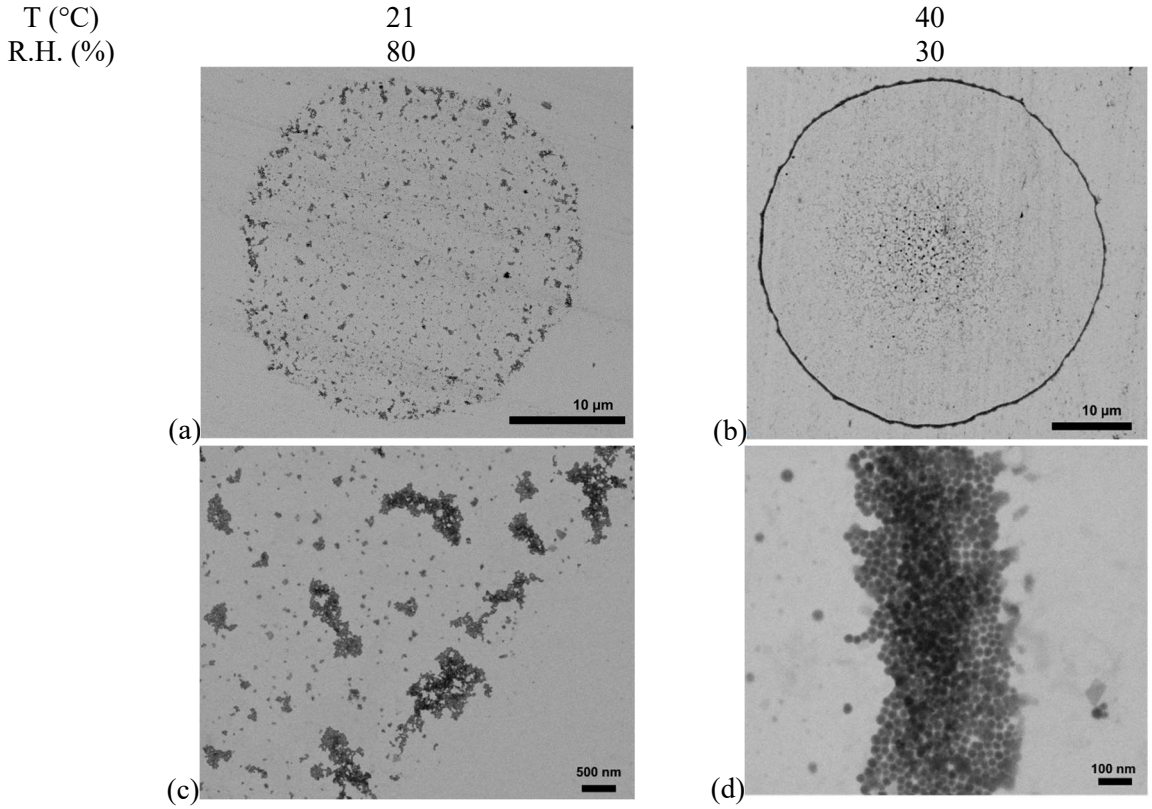

Figure 6: The effect of temperature and relative humidity on the drying patterns of SiO_2 nanoparticles printed from a suspension of $1x10^9$ NP/mL. (c) and (d) are increased magnification images of (a) and (b), respectively.

3.5. Calculation of maximum concentration for single layer

The EM images of the monolayer from printing of SiO_2 nanoparticle droplets (as seen in Figure 3(a)) were digitally analysed using the particle size distribution analysis in the ImageJ software, with the aim of determining the maximum concentration of nanoparticles in suspension which would form a monolayer in a printed droplet of a given size, and therefore the maximum nanoparticle concentration at which this method would be effective. In addition, we wished to evaluate the effectiveness of the ImageJ software for use in this method. Figure 7(a) shows the results of the automatic nanoparticle selection; most of the single particles can be distinguished and a minimum Feret diameter of approximately 20 nm can be calculated. However, the software is unable to distinguish single particles in groups/agglomerates, and therefore calculates a small number of larger particles of approximately 40 nm diameter as seen in Figure 7(b). These data were used to calculate the number of particles in the image, which was extrapolated to the number of particles in the drop size measured in these conditions (Figure 1) and correlated with the drop volume to calculate the concentration.

Two values were used in this estimate. First, for a minimum value, the simple number of particles calculated from the graphs in Figure 7 was used. A second estimate combined the number of particles in the 20 nm peak in Figure 7(b) with the number of particles in the 35 nm peak in Figure 7(b) arising from identification of groups/agglomerates multiplied by four as an estimate of the single particles in these agglomerates. The resulting estimate for the nanoparticle concentrations was in the range of 1-3 x 10^{12} NP/mL, which is higher than the concentration at which coffee rings were found in either of the images shown in Figure 3 (printed from concentrations of $1x10^{10}$ and $1x10^{11}$ NP/mL, respectively).

While this method shows promise for evaluation of nanoparticles in the monolayer, the pronounced coffee-ring effects negate the possibility of using this simple calculation for the determination of a maximum NP concentration at which a monolayer is formed.

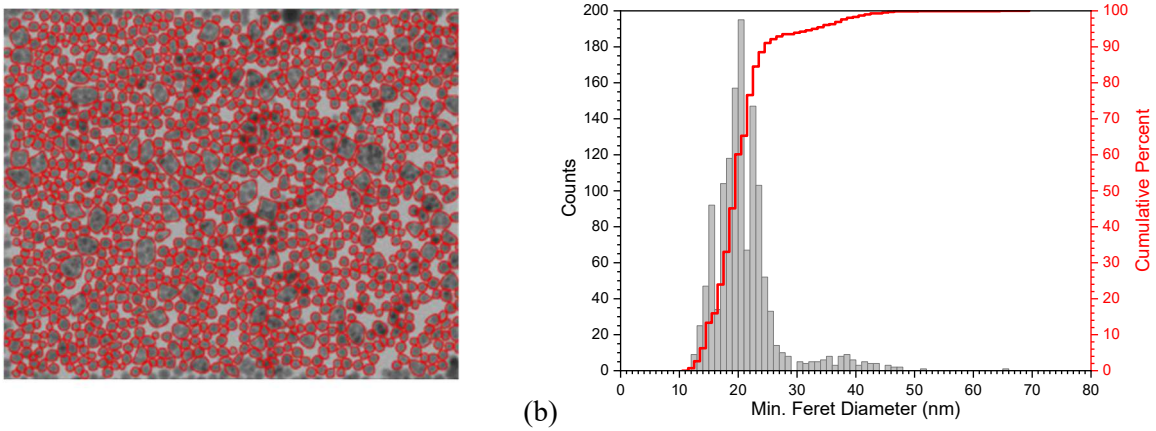

(a) (b)

Figure 7: Digital image evaluation of monolayer of SiO_2 nanoparticles

4. Conclusions and Outlook

In this publication we have demonstrated the considerations and identified the challenges for the use of microarray printing and digital image evaluation for determining the particle size distribution and concentration of nanoparticle suspensions of various materials. Results show that the process must be optimized for each individual material. While the results are promising, there are several parameters which still need to be optimized for the full implementation of this method, particularly elimination or reduction of the coffee-ring effect.

Given the sensitivity of the NanoPlotter equipment as well as the necessity to alter the particles as little as possible, the experimental conditions are available for the reduction of the coffee-ring effect are relatively limited; hence, the possibility of using alternative solvents/solutions [13,33], higher temperatures [30-32,34], freeze-drying [35] or evaporation in an alternative atmosphere [10,28,36] (e.g. ethanol vapour) as shown in literature is not available. Despite these limitations, optimization of the concentration and printing conditions for SiO_2 nanoparticles, especially temperature and humidity, are promising ways to reduce the coffee-ring and must be further investigated.

Although the gold nanoparticles could not be successfully analysed in this work due to agglomeration/aggregation, their high contrast in SEM images would mean that they may nonetheless be a good candidate for this method, particularly after purification and removal of salts from synthesis by one of the methods recently published by our group [4]. Such purification methods may also be useful for removal of surfactants from the latex nanoparticles. The contrast of the polystyrene latex nanoparticles could also potentially be increased by staining with RuO_4 which is a common method used in TEM analysis of nanostructured polymers to increase the contrast between different polymer phases.

Further work may include the use of optimized substrates for printing, in which the surface hydrophilicity/hydrophobicity is controlled by various coatings or cleaning protocols, for example treatment with plasma or UV/ozone cleaners.

5. Acknowledgements

This project has received funding from the European Union Horizon 2020 Programme (H2020) under grant agreement no. 720952. The authors thank Sigrid Benemann for SEM measurements and Dr. Christoph Hörenz for assistance with image processing.

References

[1] *ACEnano Analytical and Characterisation Excellence*, <http://www.acenano-project.eu/>
[2] Hodoroaba V-D et al. 2014 *Microsc. Microanal.* **20** 602-612
[3] Hodoroaba V-D et al 2014 *Analyst* **139** 2004-2010
[4] Bennet F et al *JoVE* 2020 **163** e61758
[5] Barmi M R and Meinhart C D *J. Phys. Chem. B* 2014 **118** 2414-2421
[6] Bromberg V et al Proceeding IMECE 2008 **68877** 17-24
[7] Hu H and Larson R G *J. Phys. Chem. B* 2006 **110** 7090-7094
[8] Hu H and Larson R G *Langmuir* 2005 **21** 3972-3980
[9] Vyas D R et al *Heat Mass Transf.* 2019 **55** 791-809
[10] Hegde Oet al *J. Colloid Interface Sci.* 2019 **541** 348-355
[11] Guha R et al *ACS Appl. Mater. Interfaces* 2017 **9** 43352-43362
[12] Gorr H M et al *Colloids Surf. B* 2013 **103** 59-66
[13] Cui L et al *ACS Appl. Mater. Interfaces* 2012 **4** 2775-2780
[14] Crivoi A et al *Proceedings* MNHMT 2013 22190
[15] Crivoi A and Duan F *Langmuir* 2013 **29** 12067-12074
[16] Bansal L et al *Appl. Phys. Lett.* 2018 **112** 2111605
[17] Al-Milaji K N and Zhao H *J Phys. Chem. C* 2019 **123** 12029-12041
[18] Mampallil D and Eral H B *Adv. Colloid Interface Sci.* 2018 **252** 38-54
[19] Michen B et al *Sci. Rep.* 2015 **5** 9793
[20] Tannenberg R et al *Imaging Microsc.* 2016 **March** 33–35.
[21] Mielke J et al *Microsc. Microanal.* 2017 **23** 163-172
[22] Kumagai K and Kurokawa A *Metrologia* 2019 **56** 044001
[23] Abdullah A A et al *Eur. J. Mech. B-Fluids* 2018 **67** 259-268
[24] Ahmad I and Jan R *Nano* 2019 **14** 14
[25] Hamptonet al *J. Colloid Interface Sci.* 2012 **377** 456-462
[26] Crivoi A and Duan F *J. Phys. Chem. B* 2013 **117** 5932-5938
[27] Ellahi R et al *Int. J. Num. Meth. Heat Fluid Flow* 2016 **26** 2160-2174
[28] Homede E and Manor O *J. Colloid Interface Sci.* 2020 **562** 102-111
[29] Schneider C A et al *Nat. Methods* 2012 **9** 671-675
[30] Zhong X and Duan F *Phys. Chem. Chem. Phys*. 2016 **18** 20664-20671
[31] Malla L K et al *Colloids Surf. A* 2020 **584** 124009
[32] Parsa M et al *J. Phys. Chem. B* 2017 **121** 11002-11017
[33] Kajiya T et al *J. Phys. Chem. B* 2009 **113** 15460-15466
[34] Thokchom A K et al *Sens. Actuators B* 2017 **252** 1063-1070
[35] Jambon-Puillet E *Langmuir* 2019 **35** 5541-5548
[36] Majumder M et al *J. Phys. Chem. B* 2012 **116** 6536-6542